Desalination and Water Treatment
www.deswater.com
1944-3994/1944-3986 © 2012 Desalination Publications. All rights reserved
doi: 10/5004/dwt.2012.2825

Taylor & Francis
Taylor & Francis Group

42 (2012) 216–221
April

Microwave-assisted synthesis of ZnO for photocatalytic reduction of Cr(VI) in aqueous solution

Xinjuan Liu[a], Tian Lv[a], Likun Pan[a,*], Zhuo Sun[a], Chang Qing Sun[b]

[a]*Engineering Research Center for Nanophotonics & Advanced Instrument, Ministry of Education, Department of Physics, East China Normal University, Shanghai, 200062 China*
Tel. +86 21 62234132; Fax: +86 21 62234321; email: lkpan@phy.ecnu.edu.cn
[b]*School of Electrical and Electronic Engineering, Nanyang Technological University, Singapore 639798, Singapore*

Received 2 June 2011; Accepted 20 December 2011

ABSTRACT

ZnO sheets have been synthesized via microwave-assisted reaction of ZnO precursor in aqueous solution using a CEM microwave system. Their morphologies, crystal structures and photocatalytic performances in the reduction of Cr(VI) were characterized using scanning electron microscopy, transmission electron microscopy, X-ray diffraction spectroscopy and UV-vis absorption spectrophotometer, respectively. Results show that ZnO sheets synthesized in 5 min time scale exhibits a optimal photocatalytic performance in the reduction of Cr(VI) with removal efficiency of 81% under UV irradiation due to the maximal intensity of light absorption and the minimal probability of electron-hole pair recombination.

Keywords: Microwave-assisted synthesis; ZnO; Sheet; Photocatalysis; Cr(VI); UV light

1. Introduction

Removal of pollutants contained heavy metals and dye from both underground and surface water supplies is increasingly demanded in water purification [1–14]. Among all heavy metals, Cr(VI) is toxic to most organisms when its concentration is above 0.05 mg l^{-1} that will cause irritation and corrosion of human skin. Cr(VI) is generally released from electroplating, leather tanning, metal finishing, dyeing, textiling, steel fabricating, paint and pigments, fertilizing, photographying, etc. Therefore, it is very important to find an effective method to remove Cr(VI) from industrial wastewaters. Methods including adsorption [15–22], biosorption [23–25], ion exchange [26,27], electrocoagulation [28–30] and membrane filtration [31–34] have been widely used for the removal of Cr(VI). However, these technologies demonstrated drawbacks, such as membrane fouling, high power consumption and expensive for operation and maintenance. Considerable attentions have been paid to semiconductor oxide photocatalysis as a novel and environmentally-friendly technology for the removal of Cr(VI) from aqueous solutions [35–39]. Among them, ZnO has been proven to be the promising photocatalyst for widespreading environmental applications due to its intriguing chemical, optical and electric properties, low cost, and ease of availability [40–45]. Yang and Chan [46] prepared nanoscale ZnO by co-precipitation method and used Alizarin Red S dye to sensitize ZnO for photocatalytic reduction of Cr(VI) and a reduction rate of 90% was achieved under the irradiation of sunlight. Chakrabarti et al. [47] showed that about 90% Cr(VI) in aqueous solutions can be effectively reduced to trivalent state using ZnO under UV irradiation. Qamar et al. [48]

*Corresponding author.

2011 Qingdao International Desalination Conference Symposium on Desalination and Water Treatment Global Platform for Water Solutions, June 20–23, 2011 Qingdao, China

demonstrated the complete removal of Cr(VI) in aqueous suspensions of ZnO nanoparticles synthesized by precipitation method using a novel laser-induced photocatalytic process without the use of any other additives. About 95% Cr(VI) was removed within a short time (60 min) of laser exposure. However, as a promising candidate for photocatalytic reduction of Cr(VI), the exploration on the potentiality of ZnO is not yet enough insofar. Especially as a cheaper, quicker, and versatile technique, microwave-assisted reaction is seldom employed to synthesize ZnO for photocatalytic application.

In this work, we successfully fabricated ZnO sheets via microwave-assisted reaction of ZnO precursor in aqueous solution using a CEM microwave system and investigated their photocatalytic performance. Microwave irradiation can heat the reactant easily to high temperatures in a short time by transferring energy selectively to microwave absorbing polar solvents. Thus it can facilitate mass production in a short time with little consumption of energy [49–51]. ZnO sheets synthesized in 5 min exhibits a optimal photocatalytic performance in reduction of Cr(VI) under UV light irradiation.

2. Experimental

2.1. Synthesis of ZnO sheets

A 20 ml 0.1 M $ZnSO_4$ solution was placed in a 35 ml microwave tube and then a dilute NaOH solution was dropped to adjust the pH = 9. Subsequently, the solution was sonicated for 30 min to produce uniform dispersion. The mixture was then put into an automated focused microwave system (Explorer-48, CEM Co.) and treated for different time at 150°C. The as-synthesized ZnO samples in 5, 10, 15, 20, and 25 min, named as Z-1, Z-2, Z-3, Z-4 and Z-5, were isolated by filtration, washed for three times with distilled water, and finally dried in a vacuum oven at 60°C for 24 h.

2.2. Characterization

The surface morphology, structure and composition of the samples were characterized using field-emission scanning electron microscopy (FESEM, Hitachi S-4800), high-resolution transmission electron microscope (HRTEM, JEOL-2010), X-ray diffraction spectroscopy (XRD, Holland Panalytical PRO PW3040/60) with Cu Kα radiation (V = 30 kV, I = 25 mA), and energy dispersive X-ray spectroscopy (EDS, JEM-2100), respectively. The UV-vis absorption spectra were recorded using a Hitachi U-3900 UV-vis spectrophotometer. Room temperature photoluminescence (PL) spectra were recorded on a HORIBA Jobin Yvon fluoromax-4 fluorescence spectrophotometer, using 340 nm excitation line of a Xe lamp as light source.

2.3. Photocatalytic experiments

The photocatalytic performance of the as-prepared samples was evaluated using photocatalytic reduction of Cr(VI) under UV light irradiation. The samples (1 g l^{-1}) were dispersed in the 60 ml Cr(VI) suspensions (10 mg l^{-1}) which were prepared by dissolving $K_2Cr_2O_7$ into deionized water. The mixed suspensions were first magnetically stirred in the dark for 0.5 h to reach the adsorption-desorption equilibrium. Stirring under the ambient conditions, the mixed suspensions were exposed to UV irradiation produced by a 500 W high-pressure Hg lamp, which emits radiation centered at various wavelengths with the main wave crest at 365 nm. At certain time intervals, 2 ml of the mixed suspensions were extracted and centrifuged to remove the photocatalyst. The filtrates were analyzed by recording UV-vis spectra of Cr(VI). The effect of various operational parameters, that is, metal ion concentration, catalyst concentration, pH, contact time of aqueous solution of metal ions on the photoreactivity of proposed catalyst also were observed. The pH was adjusted by adding 0.1 M NaOH and HCl.

The photocatalytic reaction kinetics was studied using Langmuir–Hinshelwood model. The pseudo-first-order equation is employed to fit the experimental data and can be formulated as [52]:

$$\ln(C_i/C_0) = -kt \quad (1)$$

where t and k are the photocatalysis time (min) and the reaction rate constant (min^{-1}), respectively. C_0 and C_i are the initial concentration and the concentration of Cr(VI) at time t (mg l^{-1}), respectively.

3. Results and discussion

Fig. 1(a)–(e) show the FESEM images of Z-1, Z-2, Z-3, Z-4 and Z-5. It is clearly observed that ZnO displays the sheet nanostructure and the size of sheet decreases with the increase of synthesis time. The existence of ZnO was confirmed by the presence of Zn and O peaks in the EDS data (Fig. 1(f)). Fig. 2(a) and (b) show the low- and high-magnification HRTEM images of Z-1. It gives further insight into the structural features of the ZnO sheets and the ZnO (100) spacing of 0.28 nm [53].

The XRD patterns in Fig. 3 show the excellent crystal structures of ZnO sheets. The peaks at 31.6, 34.4, 36.1, 47.3, 56.3, 62.6, and 67.6° correspond to the (100), (002), (101), (102), (110), (103), and (112) planes of ZnO. No impurities such as $Zn(OH)_2$ can be detected. All of the diffraction peaks can be well-indexed to hexagonal wurtzite crystal structure (JPCDS 36-1451), which demonstrates that the long synthesis time results in not the development of new crystal orientations or changes in preferential orientations of ZnO.

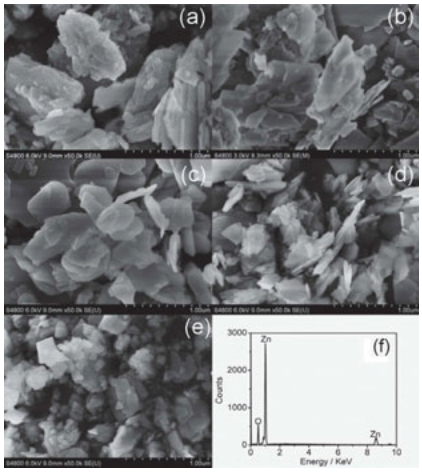

Fig. 1. FESEM images of (a) Z-1, (b) Z-2, (c) Z-3, (d) Z-4, (e) Z-5, (f) EDS spectrum of Z-1.

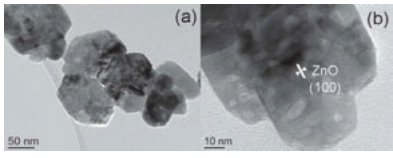

Fig. 2. (a) Low- (b) high-magnification HRTEM images of Z-1.

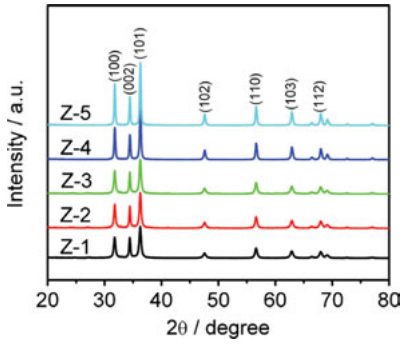

Fig. 3. XRD patterns of Z-1, Z-2, Z-3, Z-4 and Z-5.

The diffuse reflectance spectra in Fig. 4 show the sharp characteristic absorption peak at 370 nm, indicating the presence of good crystalline and impurity suppressed ZnO nanostructures [54]. The absorbance of the as-synthesized samples decreases with the increase of synthesis time without rendering energy shift. The decrease of absorbance with size reduction is related to the quantum efficiency that is lowered by the surface structural disorder [55].

As shown in Fig. 5, the PL spectra under the excitation wavelength of 340 nm exhibit strong emission at ≈380 nm, which is attributed to free-exciton recombination crossing the optical band gap of 1238 nm eV/380 nm = 3.26 eV. The slightly drop of the PL peak intensities with the decrease

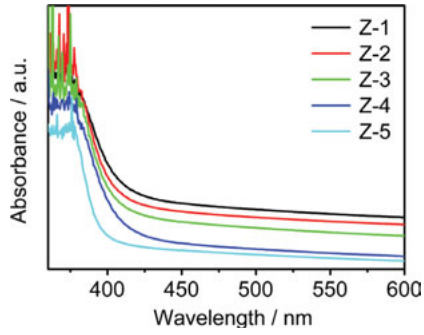

Fig. 4. Diffuse reflectance spectra of Z-1, Z-2, Z-3, Z-4 and Z-5.

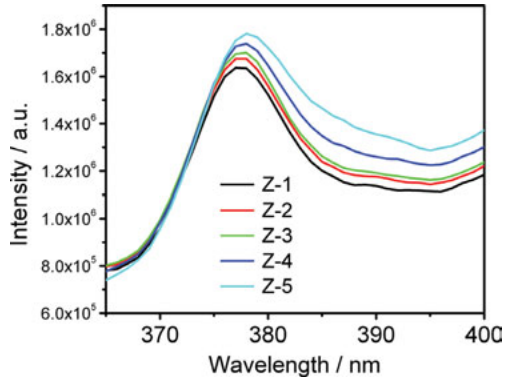

Fig. 5. PL spectra of of Z-1, Z-2, Z-3, Z-4 and Z-5 at excitation wavelength of 340 nm.

of synthesis time, indicating lower recombination rate of the photo-induced electrons and holes in the respective samples. The slight redshift of the PL peak with synthesis time indicates the growth of particle size, being agreement with the SEM data in Fig. 1.

The effect of various operational parameters, that is, catalyst concentration, pH, metal ion concentration, contact time of aqueous solution of metal ions on the photocatalytic reduction of Cr(VI) using Z-2 were tested and the results are shown in Table 1. It can be seen that (i) the removal efficiency increases from 20% to 82% with the increasing dosage of Z-2 photocatalyst from 0.5 g l^{-1} to 1.5 g l^{-1} due to the increase of the photogenerated electron-hole pairs. However, when the Z-2 amount is further increased, the photocatalytic performance deteriorates. It is because that when the photocatalyst dosage is increased above a certain value, the solution transparence is crippled and scattering effect happens. Correspondingly the light utilization rate is reduced which lowers the photocatalytic performance of

Table 1
Effect of various operational parameters, that is, catalyst concentration, pH, metal ion concentration, contact time of aqueous solution of metal ions on the photocatalytic reduction of Cr(VI) using Z-2

Catalyst concentration (g l^{-1})	Removal efficiency (%)	pH	Removal efficiency (%)	Metal ion concentration (mg l^{-1})	Removal efficiency (%)	Contact time (min)	Removal efficiency (%)
0.5	20	5	20	2.5	64	0	16
1.0	58	7	58	5	53	10	26
1.5	82	9	62	10	58	20	39
2.0	29	11	17	20	42	30	58

ZnO; (ii) the removal efficiency is significantly increased from 20% to 58% with the increase of pH value from 5 to 7 and reaches a maxim of 62% at a pH value of 9 because more Cr(VI) is absorbed onto the photocatalyst surface with negative charge. However, the degradation efficiency decreases when pH value is further increased to 11, which should be ascribed to the instability of ZnO in strong alkali condition; (iii) the removal efficiency decreases from 64% to 42% with the increase of metal Cr(VI) ion concentration from 2.5 to 20 mg l^{-1}; (iv) the removal efficiency increases from 16% to 58% with the increasing of contact time of aqueous solution from 0 to 30 min.

Fig. 6 shows the photocatalytic reduction of Cr(VI) under UV irradiation using Z-1, Z-2, Z-3, Z-4 and Z-5. It is observed that the photocatalytic performance of ZnO sheets is dependent on the synthesis time and ZnO sheets synthesized in 5 min exhibits a optimal photocatalytic performance. The removal efficiency of Cr(VI) for ZnO sheets synthesized in 5 min is 81%. However, when the synthesis time is increased, the removal efficiency decreases to 58%, 41%, 40%, 44% and 48% for Z-2, Z-3, Z-4 and Z-5, respectively. The enhanced photocatalytic performance of ZnO synthesized in short time is ascribed to the increased light absorption intensity and the decreased probability of the photoelectron-hole pair recombination.

In the photocatalytic reduction process of Cr(VI), ZnO is excited by the absorption of photon under UV irradiate and electron-hole pairs are created:

$$ZnO + h\nu \longrightarrow h^+ + e^-$$

Cr(VI) is reduced to Cr(III) by the photo-generated electrons, while the hole reaction is the oxidation of water to oxygen as follows:

$$Cr_2O_7^{2-} + 14H^+ + 6e^- \longrightarrow 2Cr^{3+} + 7H_2O$$

$$2H_2O + 4h^+ \longrightarrow O_2 + 4H^+$$

The stable final product Cr(III) is removed from the aqueous solution by precipitation in the form of $Cr(OH)_3$ [56].

Fig. 7 shows the linear fitting using the pseudo-first-order kinetic equations to the experimental data for Z-1, Z-2, Z-3, Z-4 and Z-5. The values of rate constants (k) can be obtained directly from the fitted straight-line plots of

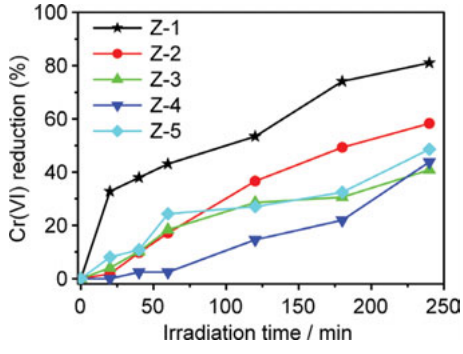

Fig. 6. Photocatalytic reduction of Cr(VI) by Z-1, Z-2, Z-3, Z-4 and Z-5 under UV irradiation. The concentrations of Cr(VI) and photocatalyst are 10 mg l^{-1} and 1 g l^{-1}, respectively.

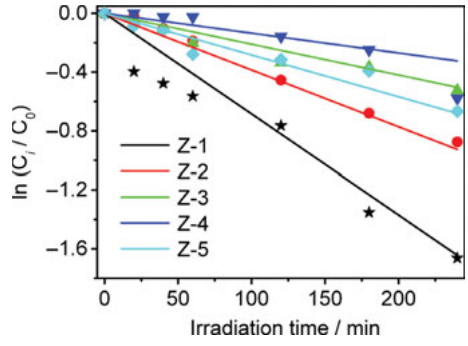

Fig. 7. Photocatalytic reaction kinetics of Cr(VI) with reaction time.

versus reaction time, which follow the order: Z-1 (0.00685 min^{-1}) > Z-2 (0.00386 min^{-1}) > Z-5 (0.00284 min^{-1}) > Z-3 (0.0021 min^{-1}) > Z-4 (0.00135 min^{-1}). Z-1 exhibits an optimal photocatalytic activity under UV irradiation. The discrepancies between model and experimental data at initial reaction time should be ascribed to the high rate constant, which is possibly related to the high Cr(VI) concentration on the surface of photocatalyst when the photocatalysis begins after dark reaction.

4. Conclusions

ZnO sheets synthesized via microwave-assisted reaction of ZnO precursor in aqueous solution using a CEM microwave system and their photocatalytic experiments showed that: (i) the photocatalytic performance of ZnO is sensitive to the synthesis time; (ii) ZnO synthesized in 5 min exhibits an optimal photocatalytic performance and Cr(VI) removal efficiency up to 81%; (iii) the enhanced photocatalytic performance of ZnO is ascribed to the increased light absorption intensity and the lowered probability of photoelectron-hole pair recombination. The difference between the absorbed and the emitted light intensities shall contribute to the photocatalytic efficiency of the material. The photocatalytic reduction using ZnO sheets may provide an alternative cheaper, efficient way for removal of Cr(VI) under UV irradiation.

Acknowledgments

Financial support from Special Project for Nanotechnology of Shanghai (No. 1052nm02700) and Large Instruments Open Foundation of East China Normal University and ECNU Reward for Excellent Doctors in Academics (No. XRZZ2011017) are gratefully acknowledged.

References

[1] C.Y. Nie, Y.K. Zhan, L.K. Pan, H.B. Li and Z. Sun, Electrosorption of different cations and anions with membrane capacitive deionization based on carbon nanotube/nanofiber electrodes and ion-exchange membranes, Desalin. Water Treat., 30 (2011) 266–271.

[2] A.M. Donia, A.A. Atia and R.T. Rashad, Fast removal of Cu(II) and Hg(II) from aqueous solutions using kaolinite containing glycidyl methacrylate resin, Desalin. Water Treat., 30 (2011) 254–265.

[3] M.T.G. Chuah, Y. Robiah, A.R. Suraya and T.S.Y. Choong, Single and binary adsorptions isotherms of Cd(II) and Zn(II) on palm kernel shell based activated carbon, Desalin. Water Treat., 29 (2011) 140–148.

[4] M. Moussavi, How mercury can simply and effectively be removed from a waste stream, Desalin. Water Treat., 28 (2011) 88–91.

[5] V.K. Gupta, R. Jain, A. Nayak, S. Agarwal and M. Shrivastava, Removal of the hazardous dye-Tartrazine by photodegradation on titanium dioxide surface, Mater. Sci. Eng. C., 31 (2011) 1062–1067.

[6] V.K. Gupta, R. Jain, S. Agarwal and M. Shrivastava, Kinetics of photo-catalytic degradation of hazardous dye Tropaeoline 000 using UV/TiO_2 in a UV reactor, Colloids Surf. A., 378 (2011) 22–26.

[7] V.K. Gupta, R. Jain, A. Mittal, M. Mathur and S. Sikarwar, Photochemical degradation of the hazardous dye Safranin-T using TiO_2 catalyst, J. Colloid Interface Sci., 309 (2007) 464–469.

[8] I. Ali and V.K. Gupta, Advances in water treatment by adsorption technology, Nat. Protoc., 1 (2007) 2661–2667.

[9] V.K. Gupta and Suhas, Application of low-cost adsorbents for dye removal-A review, J. Environ. Manage., 90 (2009) 2313–2342.

[10] V.K. Gupta, P.J.M. Carrott, M.M.L. Ribeiro Carrott and Suhas, Low-cost adsorbents: growing approach to wastewater treatment-A review, Crit. Rev. Env. Sci. Technol., 39 (2009) 783–842.

[11] V.K. Gupta and I. Ali, Removal of endosulfan and methoxychlor from water on carbon slurry, Environ. Sci. Technol., 42 (2008) 766–770.

[12] V.K. Gupta, A. Mittal, L. Kurup and J. Mittal, Adsorption of basic fuchsin using waste materials-bottom ash and de-oiled soya as adsorbents, J. Colloid Interface Sci., 319 (2008) 30–39.

[13] V.K. Gupta, R. Jain, S. Varshney and V.K. Saini, Removal of reactofix navy blue 2 GFN from aqueous solutions using adsorption techniques, J. Colloid Interface Sci., 307 (2007) 326–332.

[14] V.K. Gupta, A. Mittal, R. Jain, M. Mathur and S. Sikarwar, Adsorption of safranin-T from wastewater using waste materials—activated carbon and activated rice husks, J. Colloid Interface Sci., 303 (2006) 80–86.

[15] Y.G. Zhao, H.Y. Shen, S.D. Pan and M.Q. Hu, Synthesis, characterization and properties of ethylenediamine-functionalized Fe_3O_4 magnetic polymers for removal of Cr(VI) in wastewater, J. Hazard. Mater., 182 (2010) 295–302.

[16] P. Yuan, D. Liu, M.D. Fan, D. Yang, R.L. Zhu, F. Ge, J.X. Zhu and H.P. He, Removal of hexavalent chromium (Cr(VI)) from aqueous solutions by the diatomite-supported/unsupported magnetite nanoparticles, J. Hazard. Mater., 173 (2010) 614–621.

[17] V.K. Gupta, S. Agarwa and T.A. Saleh, Chromium removal combining the magnetic properties of iron oxide with adsorption properties of carbon nanotubes, Water Res., 45 (2011) 2207–2212.

[18] R.A.K. Rao and F. Rehman, Adsorption studies on fruits of Gular (Ficus glomerata): Removal of Cr(VI) from synthetic wastewater, J. Hazard. Mater., 181 (2010) 405–412.

[19] S. Gupta and B.V. Babu, Experimental, kinetic, equilibrium and regeneration studies for adsorption of Cr(VI) from aqueous solutions using low cost adsorbent (activated flyash), Desalin. Water Treat., 20 (2010) 168–178.

[20] M. Bansal, D. Singh and V.K. Garg, Chromium (VI) uptake from aqueous solution by adsorption onto timber industry waste, Desalin. Water Treat., 12 (2009) 238–246.

[21] I. Marzouk, C. Hannachi, L. Dammak and B. Hamrouni, Removal of chromium by adsorption on activated alumina, Desalin. Water Treat., 26 (2011) 279–286.

[22] S.S. Liu, Y.Z. Chen, D.L. Zhang, G.M. Hua, W. Xu, N. Li and Y. Zhang, Enhanced removal of trace Cr(VI) ions from aqueous solution by titanium oxide-Ag composite adsorbents, J. Hazard. Mater., 190 (2011) 723–728.

[23] G.Q. Chen, W.J. Zhang, G.M. Zeng, J.H. Huang, L. Wang and G.L. Shen, Surface-modified Phanerochaete chrysosporium as a biosorbent for Cr(VI)-contaminated wastewater, J. Hazard. Mater., 186 (2011) 2138–2143.

[24] H.J. Cui, M.L. Fu, S. Yu and M.K. Wang, Reduction and removal of Cr(VI) from aqueous solutions using modified byproducts of beer production, J. Hazard. Mater., 186 (2011) 1625–1631.

[25] A.H. Sulaymon, S.E. Ebrahim, S.M. Abdullah and T.J. Al-Musawi, Removal of lead, cadmium, and mercury ions using biosorption, Desalin. Water Treat., 24 (2011) 344–352.

[26] T. Sardohan, E. Kir, A. Gulec and Y. Cengeloglu, Removal of Cr(III) and Cr(VI) through the plasma modified and unmodified ion-exchange membranes, Sep. Purif. Technol., 74 (2010) 14–20.

[27] S. Edebali and E. Pehlivan, Evaluation of Amberlite IRA96 and Dowex 18 ion-exchange resins for the removal of Cr(VI) from aqueous solution, Chem. Eng. J., 161 (2010) 161–166.
[28] M.S. Bhatti, A.S. Reddy, R.K. Kalia and A.K. Thukral, Modeling and optimization of voltage and treatment time for electrocoagulation removal of hexavalent chromium, Desalination, 269 (2011) 157–162.
[29] M.S. Bhatti, A.S. Reddy and A.K. Thukral, Electrocoagulation removal of Cr(VI) from simulated wastewater using response surface methodology, J. Hazard. Mater., 172 (2009) 839–846.
[30] F. Akbal and S. Camci, Copper, chromium and nickel removal from metal plating wastewater by electrocoagulation, Desalination, 269 (2011) 214–222.
[31] W.D. Zhang, J.T. Liu, Z.Q. Ren, S.G. Wang, C.S. Du and J.N. Ma, Kinetic study of chromium (VI) facilitated transport through a bulk liquid membrane using tri-n-butyl phosphate as carrier, Chem. Eng. J., 150 (2009) 83–89.
[32] A.O. Acosta, C. Illanes and J. Marchese, Removal and recovery of Cr(III) with emulsion liquid membranes, Desalin. Water Treat., 7 (2009) 18–24.
[33] M. Sankir, S. Bozkir and B. Aran, Preparation and performance analysis of novel nanocomposite copolymer membranes for Cr(VI) removal from aqueous solutions, Desalination, 251 (2010) 131–136.
[34] S. Alpaydin, A. Saf, S. Bozkurt and A. Sirit, Kinetic study on removal of toxic metal Cr(VI) through a bulk liquid membrane containing p-tert-butylcalix [4] arene derivative, Desalination, 275 (2011) 166–171.
[35] A. Idris, N. Hassan, N.S. Mohd Ismail, E. Misran, N.M. Yusof, A.F. Ngomsik and A. Bee, Photocatalytic magnetic separable beads for chromium(VI) reduction, Water Res., 44 (2010) 1683–1688.
[36] J. Kuncewicz, P. Zabek, G. Stochel, Z. Stasicka and W. Macyk, Visible light driven photocatalysis in chromate (VI)/TiO_2 systems Improving stability of the photocatalyst, Catal. Today., 161 (2011) 78–83.
[37] N. Nasrallah, M. Kebir, Z. Koudri and M. Trari, Photocatalytic reduction of Cr(VI) on the novel hetero-system $CuFe_2O_4$/CdS, J. Hazard. Mater., 185 (2011) 1398–1404.
[38] X.F. Lei and X.X. Xue, Photocatalytic reduction of Cr(VI) in the presence of citric acid over perovskite type SO_4^{2-}/TBBFS under UV-vis light irradiation, Adv. Mater. Res., 113 (2010) 1632–1638.
[39] M. Kebir, M. Chabani, N. Nasrallah, A. Bensmaili and M. Trari, Coupling adsorption with photocatalysis process for the Cr(VI) removal, Desalination, 270 (2011) 166–173.
[40] D. Lin, H. Wu, R. Zhang and W. Pan, Enhanced photocatalysis of electrospun Ag-ZnO heterostructured nanofibers, Chem. Mater., 21 (2009) 3479–3484.
[41] S.F. Chen, W. Zhao, S.J. Zhang and W. Liu, Preparation, characterization and photocatalytic activity of N-containing ZnO powder, Chem. Eng. J., 148 (2009) 263–269.
[42] J.W. Li, X.J. Liu, L.W. Yang, Z.F. Zhou, G.F. Xie, Y. Pan, X.H. Wang, J. Zhou, L.T. Li, L.K. Pan, Z. Sun and C.Q. Sun, Photoluminescence and photoabsorption blueshift of nanostructured ZnO: Skin-depth quantum trapping and electron-phonon coupling, Appl. Phys. Lett., 95 (2009) 031906.
[43] A.R. Khataee and M. Zarei, Photocatalysis of a dye solution using immobilized ZnO nanoparticles combined with photoelectrochemical process, Desalination, 273 (2011) 453–460.
[44] A. Shafaei, M. Nikazar and M. Arami, Photocatalytic degradation of terephthalic acid using titania and zinc oxide photocatalysts: Comparative study, Desalination, 252 (2010) 8–16.
[45] B.H. Hameed, U.G. Akpan and K.P. Wee, Photocatalytic degradation of acid red 1 dye using ZnO catalyst in the presence and absence of silver, Desalin. Water Treat., 27 (2011) 204–209.
[46] G.C.C. Yang and S.W. Chan, Photocatalytic reduction of chromium (VI) in aqueous solution using dye-sensitized nanoscale ZnO under visible light irradiation, J. Nanopart. Res., 11 (2009) 221–230.
[47] S. Chakrabarti, B. Chaudhuri, S. Bhattacharjee, A.K. Ray and B.K. Dutta, Photo-reduction of hexavalent chromium in aqueous solution in the presence of zinc oxide as semiconductor catalyst, Chem. Eng. J., 153 (2009) 86–93.
[48] M. Qamar, M.A. Gondal and Z.H. Yamani, Laser-induced efficient reduction of Cr(VI) catalyzed by ZnO nanoparticles, J. Hazard. Mater., 187 (2011) 258–263.
[49] A.V. Murugan, T. Muraliganth and A. Manthiram, Rapid, facile microwave-solvothermal synthesis of graphene nanosheets and their polyaniline nanocomposites for energy storage, Chem. Mater., 21 (2009) 5004–5006.
[50] C.T. Lee, F.S. Chen and C.H. Lu, Microwave-assisted solvothermal synthesis and characterization of SnO_2: Eu^{3+} phosphors, J. Alloys Compd., 490 (2010) 407–411.
[51] F.Y. Jiang, C.M. Wang, Y. Fu and R.C. Liu, Synthesis of iron oxide nanocubes via microwave-assisted solvolthermal method, J. Alloy Compd., 503 (2010) L31–L33.
[52] Y. Zhang, J.C. Crittenden, D.W. Hand and D.L. Perram, Fixed-bed photocatalysts for solar decontamination of water, Environ. Sci. Technol., 28 (1994) 435–442.
[53] J.L. Wu, X.P. Shen, L.J. Jiang, K. Wang and K.M. Chen, Solvothermal synthesis and characterization of sandwich-like graphene/ZnO nanocomposites, Appl. Surf. Sci., 256 (2010) 2826–2830.
[54] J. Lin, M. Penchev, G. Wang, R.K. Paul, J.B. Zhong, X.Y. Jing, M. Ozkan and C.S. Ozkan, Heterogeneous graphene nanostructures: ZnO nanostructures grown on large-area graphene layers, Small, 6 (2010) 2448–2452.
[55] R.A. Street, Hydrogenated amorphous silicon (Cambridge University Press, 1991).
[56] D.W. Chen and A.K. Ray, Removal of toxic metal ions from wastewater by semiconductor photocatalysis, Chem. Eng. Sci., 56 (2001) 1561–1570.